

**ELECTROCHEMICAL AND RADIO FREQUENCY  
SPUTTERING GROWTH OF GaN  
NANOSTRUCTURES ON  
POROUS SILICON**

**SITI NUR ATIKAH BINTI SHAMSUDDIN**

**UNIVERSITI SAINS MALAYSIA**

**2019**

**ELECTROCHEMICAL AND RADIO FREQUENCY  
SPUTTERING GROWTH OF GaN  
NANOSTRUCTURES ON  
POROUS SILICON**

by

**SITI NUR ATIKAH BINTI SHAMSUDDIN**

**Thesis submitted in fulfillment of requirements  
for the degree of  
Master of Science**

**November 2019**

## **ACKNOWLEDGEMENT**

“All praises and thank to ALLAH”

I would like to express my deepest gratitude to my supervisor, Professor Dr. Md. Roslan Hashim for his guidance, intellectual support, and inspiring words.

I would also like to express my appreciation to the staff in the Nano-Optoelectronics & Research Laboratory (NOR Lab), especially Mrs. Ee Bee Choo, Mr. Anas Ahmad, Mr. Abdul Jamil Yusuf, and Mr. Yushamdan Yusof, for their technical assistance and excellent hospitality. My gratitude also goes to the assistance from the staff of the Institute of Nano Optoelectronics Research and Technology (INOR) and also Solid State Physics laboratory and Clean Room laboratory, School of Physics.

I would like to thank my family for their understanding, patience and moral support all the way till the completion of my research. My deepest appreciation for my late father, Mr. Shamsuddin Mahmood, my lovely mother, Mrs. Hasnah Awang and my siblings for their love and moral support. For my husband, Mr. Muhammad Rosmizi Ramli, thank you for your understanding, patience and support.

Finally, to all my friends, thank you for all your comments, support and guidance through this journey. You all are the best!

## TABLE OF CONTENTS

<b>ACKNOWLEDGEMENT</b>	ii
<b>TABLE OF CONTENTS</b>	iii
<b>LIST OF TABLES</b>	vii
<b>LIST OF FIGURES</b>	ix
<b>LIST OF SYMBOLS</b>	xii
<b>LIST OF ABBREVIATIONS</b>	xiii
<b>ABSTRAK</b>	xv
<b>ABSTRACT</b>	xvii
<b>CHAPTER 1 - INTRODUCTION</b>	1
1.1 Introduction	1
1.2 Problem Statement	3
1.3 Research Objectives	5
1.4 Outline of Thesis	5
<b>CHAPTER 2 - LITERATURE REVIEW</b>	7
2.1 Introduction	7
2.2 Overview of Silicon Nanomaterials	7
2.3 Overview of Porous Silicon	8
2.4 Overview of GaN	11
2.5 Principles of Electrochemical Etching	15
2.5.1 Electrochemical Etching Mechanism of Porous Silicon	16

2.5.1(a) Direct Current Etching	19
2.5.1(b) Pulsed Current Etching	21
2.6 Principles of Electrochemical Deposition (ECD)	23
2.6.1 Electrodeposition of Semiconductors	24
2.7 Mechanism of Electrochemical Deposition of GaN	26
2.8 Radio Frequency (RF) Sputtering Deposition of GaN	27
2.9 Nitridation Process	28
2.10 Summary	29
<b>CHAPTER 3 - METHODOLOGY AND INSTRUMENTATION</b>	<b>30</b>
3.1 Introduction	30
3.2 Fabrication of Porous Silicon (PSi)	30
3.2.1 Preparation of Substrates	32
3.2.1(a) Wafer Cleaning	32
3.2.2 Electrochemical Etching Cell	33
3.2.3 Formation of Porous Silicon	34
3.3 Electrochemical Deposition of GaN on PSi	35
3.3.1 Preparation of Electrolyte	36
3.3.2 Preparation of Substrate	36
3.3.3 Electrochemical Deposition Cell	36
3.3.4 Growth of GaN using ECD Techniques	37
3.3.4(a) Different Durations	37
3.4 Growth of GaN using RF Sputtering	38
3.4.1 Growth of GaN on PSi Substrate	39
3.5 Thermal Annealing Process	40
3.6 Nitridation with Ammonia Gas	41

3.7 Instrumentation	42
3.7.1 X-ray Diffraction (XRD)	42
3.7.2 Field Emission Scanning Electron Microscope (FESEM) and Energy Dispersive X-ray Spectroscopy (EDX) Analysis	44
3.7.3 Raman Spectroscopy	45
3.8 Summary	46
<b>CHAPTER 4 - RESULTS AND DISCUSSION</b>	47
4.1 Introduction	47
4.2 Effect of Different Anodization Etching Parameters on the Porosity of PSi	47
4.2.1 Surface Morphology	48
4.2.2 Raman Analysis	51
4.3 Deposition of GaN by ECD Method with Different Durations	54
4.3.1 Surface Morphology	54
4.3.2 XRD Results	56
4.3.3 Raman Analysis	58
4.4 Effects of Nitridation on the Properties of GaN Thin Films Grown by ECD Technique	59
4.4.1 Surface Morphology	59
4.4.2 XRD Results	61
4.4.3 Raman Analysis	63
4.5 Growth of GaN Thin Films by RF Sputtering Technique	65
4.5.1 Surface Morphology	65
4.5.2 XRD Results	67
4.5.3 Raman Analysis	69
4.6 Growth of GaN Thin Films by RF Sputtering Technique with Different Substrates	71
4.6.1 Surface Morphology	72

4.6.2 XRD Results	73
4.6.3 Raman Analysis	75
4.7 Summary	78
<b>CHAPTER 5 - CONCLUSIONS AND RECOMMENDATIONS</b>	80
<b>REFERENCES</b>	82
<b>APPENDIX</b>	
<b>LIST OF PUBLICATION</b>	

## LIST OF TABLES

		<b>Page</b>
Table 2.1	Physical properties of both hexagonal and cubic GaN (Church et al., 2018, Menniger et al., 1996, (Kukushkin et al., 2008)	13
Table 2.2	Enthalpies of some Si-X bonds.	18
Table 2.3	Effects of anodization parameter on PSi formation (Bisi et al., 2000).	20
Table 3.1	PSi samples prepared using direct and pulse electrochemical etching method.	35
Table 3.2	GaN samples deposited on PSi using ECD method at different durations of 6, 12, 24, and 48 hours.	38
Table 4.1	PSi was prepared at pulsed etching method with different pause time, $T_{off}$ 4, 6, and 8 ms and direct current as a comparison (PS1).	49
Table 4.2	Intensity, full width half maximum (FWHM), and Raman shift for samples i.e., PS1, PS2, PS3, and PS4.	54
Table 4.3	EDX analysis results for GaN thin films deposited on PSi substrate at different time durations (a) 6 h, (b) 12 h, (c) 24 h, and (d) 48 h.	57
Table 4.4	EDX analysis results of GaN thin films deposited on PSi substrate (a) before nitridation and (b) after nitridation process.	61
Table 4.5	XRD results of GaN thin film after nitridation process.	63
Table 4.6	$E_2$ (high) and $A_1$ (LO) Raman modes of GaN thin film grown on PSi.	65
Table 4.7	XRD data of GaN peaks for sample B.	69
Table 4.8	Raman results of GaN thin films before (sample A) and after (sample B) the nitridation process.	72
Table 4.9	EDX analysis of GaN layers deposited on a different templates (a) PSi of DC (b) PSi of PC at $T_{off} = 4$ ms.	74



Table 4.10	XRD data of GaN peaks for sample (a).	76
Table 4.11	XRD data of GaN peaks for sample (b).	76
Table 4.12	Raman results of GaN thin layers deposited on a different template (a) PSi etch at DC (b) PSi etch at PC of $T_{\text{off}} = 4$ ms.	79

## LIST OF FIGURES

		<b>Page</b>
Figure 2.1	Raman spectrum of strain-free Si. The expected variation of the peak position with uniaxial compressive and tensile stresses were also indicated (Li et al., 2010).	10
Figure 2.2	Hexagonal wurtzite crystal structure of GaN. The full circles are N, and open circles are Ga atoms. Adapted from (Edgar, 1994).	12
Figure 2.3	Zinc-blende crystal structures of GaN. The full circles are N, and open circles are Ga atoms. Adapted from (Edgar, 1994).	12
Figure 2.4	Basis sequence of P <i>Si</i> formation.	21
Figure 2.5	Schematic diagram of the waveform of the pulse current used in the etching process.	23
Figure 3.1	Flow of the research methodology involved in this project.	31
Figure 3.2	(a) Diamond scribe system used to cut the Si substrate and (b) Si substrate after the cutting process (10 mm x 10 mm).	32
Figure 3.3	Accessories and compartment for etching process.	33
Figure 3.4	Schematic diagram of the etching technique.	35
Figure 3.5	Schematic diagram of the electrochemical deposition technique.	37
Figure 3.6	Schematic diagram for RF sputtering system used in this work.	39
Figure 3.7	The tube furnace (model: Lenton VTF/12/60/700) that was used in the thermal annealing process.	40
Figure 3.8	Tube furnace (Carbolite and Nabertherm) used for the nitridation process under ammonia gas.	41
Figure 3.9	High resolution of XRD system.	42

Figure 3.10	FESEM with EDX system.	45
Figure 3.11	Raman spectroscopy system used to characterize the optical properties of all samples.	46
Figure 4.1	FESEM images of surface morphology and cross-sectional of FESEM images PSi samples: PS1 formed using direct current and samples PS2-PS4 pulse etching method with different pause times $T_{off}$ 4, 6, and 8 ms.	50
Figure 4.2	Raman spectra of PSi samples etched with pulsed current for 30 min with peak current density $20 \text{ mA/cm}^2$ , cycle time $T$ of 14 ms but at different $T_{off}$ at 4, 6, and 8 ms. Raman spectrum for n-Si wafer and PSi sample (PS1) etched with direct current electrochemical etching technique was also shown.	53
Figure 4.3	FESEM images of GaN thin films deposited under different durations: (a) 6 h, (b) 12 h, (c) 24 h, (d) 48 h. Keeping at constant current density $J= 2.5 \text{ mA/cm}^2$ .	55
Figure 4.4	Atomic mass percentage of N element for GaN thin films deposited on PSi substrate at different time durations (a) 6 h, (b) 12 h, (c) 24 h, and (d) 48 h.	56
Figure 4.5	XRD patterns of the GaN deposited under different durations: (a) 6 h, (b) 12 h, (c) 24 h, and (d) 48 h with constant current density of $J= 2.5 \text{ mA/cm}^2$ .	57
Figure 4.6	Raman spectra of the four GaN thin films deposited under different durations of 6, 12, 24, and 48 hours with constant current density of $J= 2.5 \text{ mA/cm}^2$ .	58
Figure 4.7	FESEM images of GaN thin film deposited on a PSi substrate (a) before nitridation and (b) after nitridation by ECD technique.	60
Figure 4.8	XRD pattern of GaN thin film grown under nitridation technique of 400 sccm, at temperature of $950^\circ\text{C}$ for 1 hour.	61
Figure 4.9	Raman spectrum of GaN thin film grown under nitridation technique of 400 sccm, and nitridation at temperature of $950^\circ\text{C}$ for 1 hour.	63

Figure 4.10	FESEM image of GaN layers deposited on the PSi substrate by RF sputtering before nitridation (sample A) and after nitridation (sample B) process.	66
Figure 4.11	EDX results of the GaN deposited on a PSi substrate by RF sputtering before nitridation (sample A) and after nitridation (sample B) process.	67
Figure 4.12	XRD patterns of the deposited GaN layer before (sample A) and after nitridation process (sample B).	68
Figure 4.13	Raman spectra of the GaN film deposited before (sample A) and after nitridation process (sample B).	70
Figure 4.14	FESEM images of GaN layers deposited on a different templates (a) PSi of DC (b) PSi of PC at $T_{\text{off}} = 4$ ms.	73
Figure 4.15	XRD patterns of deposited GaN thin layers deposited on a different templates (a) PSi etched with DC, (b) PSi etched with PC with $T_{\text{off}} = 4$ ms.	74
Figure 4.16	Raman spectra GaN thin layers deposited on a different template (a) PSi etch at DC (b) PSi etch at PC of $T_{\text{off}} = 4$ ms.	76

## LIST OF SYMBOLS

$\theta$	Bragg's law
$\beta$	Full width half maximum (FWHM)
$h^+$	Holes
$d$	Interplanar spacing of the crystal planes
$a, b, c$	Lattice constants
$a_o$	Lattice constant in $a$ -axis of bulk material
$c_o$	Lattice constant in $c$ -axis of bulk material
$M^{Z+}$	Metal ions
$hkl$	Miller indices
$z$	Oxidation number
$k$	Scherrer's constant
$\mathcal{E}_a$	Strain along $a$ -axis
$\mathcal{E}_c$	Strain along $c$ -axis
$t$	Time
$\lambda$	Wavelength

## LIST OF ABBREVIATIONS

AC	Alternating current
a.u	Arbitrary unit
CVD	Chemical vapour deposition
I	Current
J	Current density
D	Crystallite size
T	Cycle time
DC	Direct current
E-beam	Electron beam evaporator
ECD	Electrochemical deposition
EDX	Energy dispersive X-ray
FESEM	Field emission scanning electron microscopy
FWHM	Full width at half maximum
hcp	Hexagonal closed packed
h-GaN	Hexagonal GaN plane
HVPE	Hydride vapor phase epitaxy
ICDD	International centre for diffraction data
LEDs	Light emitting diodes
MOCVD	Metal-organic chemical vapor deposition
MOVPE	Metal-organic vapour phase epitaxy
MBE	Molecular beam epitaxy
PSi	Porous Silicon
T <sub>off</sub>	Pause time

RF	Radio frequency
A <sub>1</sub> (TO)	Raman active mode
A <sub>1</sub> (LO)	Raman active mode
E <sub>1</sub> (TO)	Raman active mode
E <sub>2</sub> (high)	Raman active mode
E <sub>2</sub> (low)	Raman active mode
T	Temperature
T <sub>on</sub>	Time on
UV	Ultraviolet
VLS	Vapour-liquid-solid
XRD	X-ray diffraction

**PENUMBUHAN NANOSTRUKTUR GaN DI ATAS SILIKON BERLIANG  
MENGUNAKAN TEKNIK ELEKTROKIMIA DAN PERCIKAN  
FREKUENSI RADIO**

**ABSTRAK**

Kajian ini menumpukan perhatian kepada penumbuhan dan pencirian nanostruktur galium nitrida (GaN) yang dimendapkan ke atas substrat silikon berliang jenis-n PSi (100) dengan menggunakan teknik pemendapan elektrokimia (ECD) dan percikan frekuensi dan radio (RF). Dalam langkah pertama kerja ini, substrat PSi telah dihasilkan dengan menggunakan teknik punaran elektrokimia arus terus (DC) dan arus denyut (PC). Keputusan menunjukkan bahawa teknik punaran PC telah menghasilkan substrat PSi yang berkeliangan tinggi dan lebih seragam berbanding teknik punaran DC. Dalam langkah kedua, lapisan GaN ditumbuhkan di atas substrat silikon berliang dengan kaedah ECD. Kualiti GaN telah ditambah baik dengan proses nitridasi. Beberapa puncak GaN wurtzit heksagonal (h-GaN) telah dihasilkan pada  $32.4^\circ$ ,  $34.6^\circ$  dan  $36.8^\circ$  masing-masing bersepadanan dengan orientasi (010), (002) dan (101). Dalam kajian ini, keputusan Raman menunjukkan bahawa filem nipis GaN telah tertakluk kepada tekanan mampatan dengan merujuk kepada nilai puncak  $E_2(\text{tinggi})$  pada  $568.0 \text{ cm}^{-1}$ . Akhir sekali, lapisan GaN telah ditumbuhkan di atas PSi dengan menggunakan teknik percikan RF dan kemudian telah disepuh lindapkan dengan gas ammonia untuk menambahbaik kualiti GaN. Dari imej FESEM, lapisan GaN yang ditumbuh oleh percikan RF memperlihatkan permukaannya yang lebih licin. Puncak XRD telah menunjukkan bahawa fasa h-GaN telah dikesan pada orientasi (100), (002), (101), (102) dan (110). Sementara itu, spektrum Raman menunjukkan kehadiran mod fonon h-GaN  $E_2(\text{tinggi})$  dan  $A_1(\text{LO})$  masing-masing



pada  $568.3 \text{ cm}^{-1}$  and  $733.2 \text{ cm}^{-1}$ . Ini merupakan persetujuan yang baik / sejajar dengan peraturan pemilihan Raman untuk GaN wurtzit. Dari semua hasil, lapisan GaN yang telah ditumbuhkan melalui teknik percikan RF telah menunjukkan keputusan yang lebih baik berbanding GaN yang ditumbuhkan melalui teknik ECD.

# **ELECTROCHEMICAL AND RADIO FREQUENCY SPUTTERING GROWTH OF GaN NANOSTRUCTURES ON POROUS SILICON**

## **ABSTRACT**

This study focuses on the growth and characterization of gallium nitride (GaN) nanostructures deposited on n-type PSi (100) substrate using electrochemical deposition (ECD) and radio frequency (RF) sputtering techniques. In the first step of this work, PSi substrates were obtained using direct current (DC) and pulsed current (PC) electrochemical etching techniques. The result showed that PC etching technique produced higher porosity and more uniform PSi substrate compared to than DC etching technique. In the second step, GaN layer was grown on PSi substrate by ECD technique. The quality of GaN was improved by nitridation process. Several peaks of hexagonal wurtzite (h-GaN) were observed at  $32.4^\circ$ ,  $34.6^\circ$ , and  $36.8^\circ$  which corresponding to the (010), (002), and (101) orientations, respectively. In this study, Raman result shows that the GaN thin film was subjected to the compressive stress by referring to the value of peak  $E_2(\text{high})$  mode at  $568.0\text{ cm}^{-1}$ . Finally, GaN layer was grown on PSi by RF sputtering technique and annealed with ammonia in order to improve the crystalline quality of GaN. From the FESEM images, GaN layers grown by RF sputtering shows smoother surface. XRD peaks show that h-GaN phase was detected at (100), (002), (101), (102), and (110) orientations. Meanwhile, Raman spectra indicated the presence of h-GaN phonon modes  $E_2(\text{high})$  and  $A_1(\text{LO})$  at  $568.3\text{ cm}^{-1}$  and  $733.2\text{ cm}^{-1}$ , respectively. This is in good agreement / aligned with the Raman selection rule for wurtzite GaN. From all the results, GaN layers grown by RF sputtering technique shows better results than GaN grown with ECD technique.

# CHAPTER 1

## INTRODUCTION

### 1.1 Introduction

III-V nitrides semiconductor has become an attractive materials due to special electronic and optical products. This has make the nitrides semiconductor becomes more desirable in applications of optoelectronic devices (Carlo, 2001; Arakawa, 2002). Among these nitride compounds, GaN being a bright potential in field of semiconductor electrical and optical devices, due to its direct band gap energy of 3.4 eV. GaN is also a very attractive material for in high temperature and powerful electronic devices. This is because of its fascinating material properties such as well thermal conductivity, mechanical resistance, and high thermal stability (Akasaki & Amano, 1997).

GaN has been successfully grown on various kinds of substrates such as sapphire, silicon carbide (SiC), and silicon (Si). Generally, GaN was grown on sapphire or SiC substrates. However, these substrates are expensive and not useable in large wafer size (Pal & Jacob, 2004). Moreover, SiC substrate is considered friendlier based on thermal and electrical thoughtfulness's, but it is a bad option for light application because it is not an ultraviolet (UV) transparent and the substrate also comparatively high price. Likened to the sapphire and SiC substrates, Si substrate seems to be a flexible and efficient solution due to its low cost, good thermal conductivity and its availability in large size (Chuang et al., 2007; Mo et al., 2005).

However, there are some issues related to the growth of GaN on Si substrate. With a large lattice mismatch (17%) and a large difference of heat expansion coefficient ( $>100\%$ ), these problems make GaN difficult to grow on Si (Moram, et al., 2010). So, porous silicon (PSi) was suggested as it is an alternative choice to reduce lattice mismatch GaN/Si heteroepitaxy. This porous substrate will keep its crystalline character and has a porous structure that can help to reduce the thermal strain and to restrict the dislocations and cracks in GaN (Boufaden et al., 2003, Chaaben et al., 2004). By using radio frequency (RF) sputtering and electron beam (e-beam) evaporator, (Samsudin, 2016) has reported that the GaN thin films were successfully grown on PSi substrate by using these two techniques. The author found that PSi provides better GaN growth because it can reduce the large lattice mismatch between GaN and Si substrate.

The conventional growth techniques for GaN layer on Si substrate include molecular beam epitaxy (MBE) (Sienz, et al, 2004), metal-organic chemical vapor (MOCVD) (Puchinger et al., 2001), and hydride vapor phase (HVPE) (Kim et al., 1998). Despite of great systems, these techniques were expensive and have complicated systems. These systems need high operating cost and extraordinary care. Meanwhile, RF sputtering and electrochemical deposition (ECD) techniques are the easiest, most convenient and comparatively inexpensive as compared to the mentioned techniques. When GaN thin films can be grown using simple and inexpensive techniques like RF sputtering and ECD techniques, it would open more explorations that lead to the development of GaN technology.

## 1.2 Problem Statement

Conventional growth techniques for GaN are MBE, MOCVD, and MOVPE. Even though these techniques are able to produce good quality of GaN thin films, but these techniques are complicated and required high production cost. So, in this work, RF sputtering and ECD techniques have been chosen to grow GaN nanostructures because due to its simplicity and cost effectiveness. However, during the growth process, good qualities of GaN thin films were very hard to obtain. The deposition rates are very low and it is hard to produce high performance of GaN thin films. So, in order to improve the properties and crystalline quality of GaN thin films, nitridation process with ammonia ambient were introduced (Ghazali, et al., 2014; Samsudin, 2016).

Typically, GaN materials are grown on substrates such as sapphire and SiC. However, these substrates are either insulating or very expensive and not available in large diameters. Alternatively, Si is used as a substrate because it is inexpensive and available in large size. However, there are several difficulties for the growth of GaN on Si substrate; namely, there is a large lattice mismatch and thermal expansion coefficients between GaN and Si. To overcome these problems, PSi substrate was used.

A group of worker studied on the growth of GaN film on PSi (111) substrate using MOCVD (Jin, et al., 2016). When adjusting the depth and structure of the porous layer, the results shown that PSi with high porosity and thick porous layer can remarkably reduce cracks and improve crystal quality of the epitaxial GaN layer. For RF sputtering growth of GaN on PSi (100) and non-PSi substrates, the XRD data showed that GaN layers were grown in the hexagonal GaN (1010) orientation and

crystallized in a single crystal structure and it was found that the PSi substrates helped to reduce the defect density in GaN/Si. However, the PSi substrates were fabricated using DC electrochemical etching technique (Samsudin, et al., 2014).

Generally, PSi can be fabricated by using DC and PC electrochemical etching techniques (Xuan, et al., 2001; Wahab, et al., 2017). It was reported that PSi fabricated using PC technique exhibited more uniformity of porous structure as compared to DC technique. Ali, et al., (2008) reported this technique to fabricate PSi substrates using PC anodic etching. This technique offers the possibility of fabricating luminescent material with selective emission wavelength depending on the cycle time (T) and pause time ( $T_{off}$ ) of PC during the etching process. Raman scattering of the optical phonon in PSi showed the redshift, broadening and increased asymmetry of the Raman mode with increasing of pause time. Amran, et al., (2012) reported on the growth of gold (Au) nanoparticles effects on PSi substrate fabricated by a PC technique. The effects of pulse time  $T_{off}$  on PSi substrates were investigated. They found that, a uniform pores distribution was observed with high visible photoluminescence (PL) intensity when  $T_{off}$  was increased up to 4 ms for cycle time 14 ms. With the optimum pause time (4ms), highest light emission and the smaller crystallite size were obtained. These results indicated that the PC technique can improve the porosity of PSi substrate.

In this work, GaN nanostructures were grown on PSi substrates using ECD and RF sputtering techniques. This is the first time where PSi substrate fabricated using PC electrochemical etching techniques was used as an intermediate layer for the growth of GaN nanostructures.

### **1.3 Research Objectives**

1. To study the fabrication of PSi structure by electrochemical pulse anodic etching method.
2. To study the growth of GaN nanostructures on PSi via ECD technique.
3. To study the growth of GaN nanostructures on PSi via RF sputtering technique.

### **1.4 Outline of Thesis**

The outline of the thesis can be summarized as the following:

Chapter 1: This chapter will explain the overview of the research study. The introduction, problem statement, research objectives and the outline of the thesis will be presented.

Chapter 2: The overall literature review of electrochemical etching of PSi will be presented. The principles and mechanism of GaN growth by ECD will also be discussed and the principles of RF Sputtering techniques will be explained in this chapter.

Chapter 3: This chapter will describe the details of the methodology and instrumentation involved in this study.

Chapter 4: All the data and measurements obtained from this study will be analyzed and discussed in this chapter. Fabrication of PSi using DC and PC electrochemical etching techniques will be presented and discussed. The data and all analyses of GaN deposition thin films grown by ECD and RF sputtering techniques will be presented and discussed. The effects of nitridation process on the properties GaN thin film also will be studied and discussed.

Chapter 5: Lastly, the conclusions and the recommendations for future studies will be presented.



## CHAPTER 2

### LITERATURE REVIEW

#### 2.1 Introduction

In this chapter, all the principles and theories that have been used will be discussed. This chapter begins with a basic knowledge and information about silicon. The basic knowledge about GaN material also will be discussed. Then, the fundamental of electrochemical etching and the formation of PSi will be discussed and explained. Next, the principles of electrochemical deposition and the mechanism of gallium nitride formation are also addressed. A brief review of RF sputtering deposition technique will be presented at the end of the chapter.

#### 2.2 Overview of Silicon Nanomaterials

Silicon nanomaterial is an important type of nanomaterial, which presents special optical, electronic, and mechanical behaviors. Advance growth of Si nanomaterial is hugely encouraging the forward motion of Si nanotechnology. Increasingly fast progression of nanotechnology encouraged constant and continuous inventing functional nanomaterial. Si would be a potential substrate for the nitride (Zainal et al., 2012), where it has been found to present a number of special merits such as having noble electronic, mechanical, and optical properties; with vast surface-to-volume ratios, and superficial surface modification (Negro, et al., 2001). Silicon is a main semiconductor material and leads the recent manufacturing and production. Nonetheless, the growing miniaturization of microelectronics and growth optical communication technology industry eventually extended to the limitations of silicon technology.

Nowadays, Si has attracted great attention for the growth of epitaxial nitride for the III-V groups such as GaN, InN, and AlN. Si substrate for epitaxial growth has some benefits compared to other substrates as it can be easily obtainable with large surfaces, great crystalline perfection and at low cost (Strite & Morkoc, 1992).

### **2.3 Overview of Porous Silicon**

PSi is a promising material for device applications. Uhlir and his wife discovered this material when they are working at Bell Laboratories in the mid 1950's (Uhlir & JR., 1956). To date, PSi wafers are prepared using electrochemical method used in microelectronic circuits (Chudley & Greeno, 2012).

PSi has unique properties such as high specific surface area, high tendency for oxidation/reduction reaction and capability for surface functionalization (Ensafi, et al., 2016). Because of this it has been considered as a promising material for optoelectronic and sensor applications in the comparison to the bulk materials. Furthermore, PSi also can be used as a buffer or intermediate layer in order to minimize strain during the epitaxial growth process. By using PSi substrate, the defects in the epitaxial layer can be reduced and leads to high quality and stress-free of GaN thin films on the porous layer (Ramizy, et al., 2011). Moreover, PSi is an ideal substrate for chemical sensor applications. Owing to its low cost, easy to fabricate and easy to use along with other materials. In addition, PSi is a composed of skeleton system penetrated by a combination of pores and large surface area can be obtained. Since the PSi structure is like a sponge, it can also be seen as a quantum sponge (Bisi et al., 2000; Korotcenkov et al., 2010). Due to its sponge structure, the quantum effect acts as a basic role and it can absorb the chemical mixture of hydrofluoric acid (HF) based solution (Al-Douri et al., 2017). The large PSi surface

area is found to be a useful structural model for crystalline silicon surfaces in spectroscopic studies (Ensafi et al., 2016; Harraz, 2014; Riahi et al., 2017).

As it involves lower costs and has high specific surface area, PSi was regarded as an engineering materials that suitable for use in the chemical sensor applications (Naderi & Hashim, 2012). The size and shape of nanocrystal are practically two parameters of its optical transition energy. The energy gap between the valance and the conduction band is very important in semiconductor properties. The change in the gap between the valance and conduction bands will change the physical and chemical properties of the material (Alivisatos et al., 2007). Therefore, when the bulk size is decreased, then the quantum confined effects will increase to the nanometer length scale under the Bohr exciton radius of the semiconductor. PSi is more easily produced in HF, which can lead to higher photoluminescence at shorter wavelength. This is generally known as quantum confinement effect (Canham, 1990) where the gap of the Si band gap becomes larger and the light emission shifts to shorter wavelength due to the breaking of the conversation of momentum rule.

In 2010, (Li et al., 2010) found that the intrinsic and/or residual stress always present in the PSi layer that fabricated through chemical or electrochemical method. During the fabrication of PSi, such residual stress may induce cracks and collapsation inside the PSi structure. Thus, it is important to investigate the residual stress in PSi structure. Several techniques have been used to characterize residual stresses in PSi structure such as substrate curvature method, X-ray diffraction and Micro-Raman spectroscopy (Kraft et al., 2000; Li et al., 2010). Recently, the residual stress measurement method based on Micro-Raman spectroscopy becomes a remarkable development. There is a relationship between the stress and Raman

scattering peak. Typically, the stress can be deduced from the shift of the Raman peak position. Hence, this technique has been applied to measure the stress of PSi structure. The spectrum of Raman scattering is composed of a few characteristic peaks:  $A_1(\text{TO})$ ,  $A_1(\text{LO})$ ,  $E_1(\text{TO})$ ,  $E_1(\text{LO})$ ,  $E_2(\text{high})$  and  $E_2(\text{low})$  (Xiang, 2007). The characteristic peaks were corresponding to all the Raman-visible phonon modes. The vibration energy of its phonon mode determined the location of each Raman peak. The Raman spectrum of strain-free of bulk Si contains single peak at about  $520\text{ cm}^{-1}$  (Figure 2.1). When the lattice is in tensile or compressive, the location will shift to lower or higher frequencies, respectively. The strain and stress can be measured by detecting the Raman shift of the sample.

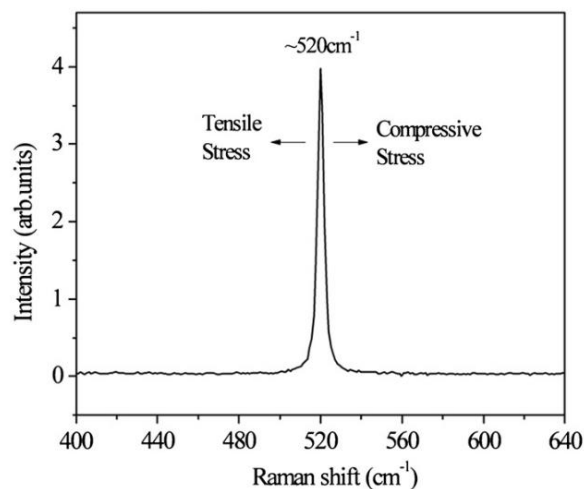


Figure 2.1 Raman spectrum of strain-free Si. The expected variation of the peak position with uniaxial compressive and tensile stresses were also indicated (Li et al., 2010).

## 2.4 Overview of GaN

GaN is a one of the direct and wide band gap semiconductor (3.4 eV) that possesses unique characteristics and has been identified as a promising semiconductor material for the use of blue and ultraviolet wavelengths optical devices (Hasegawa & Sato, 2005). These characteristics are beneficial for the creation of efficient optoelectronic and power devices (Yam, et al., 2009). With large band gap and chemical stability, GaN is also an attractive material for high temperature and electronic devices (Reddy et al., 2008).

GaN has two structural forms, which is hexagonal wurtzite and cubic zinc-blende structures. Both structures provide different lattice parameters, and leads to different fundamental properties of nitride materials. GaN can normally be formed in the structure of hexagonal wurtzite, due to the stable phase structure. There are two lattice constants, symbolized as  $a$  and  $c$  in the hexagonal close-packed unit. Instead, the atoms are arranged in the same distance as the high crystal symmetry (so-called face-centered cubic) in the cubic structure, which means cubic cell has a single lattice constant,  $a$ . Each atom of Ga and N in both crystal structures is tetrahedral and coordinated with four atoms with different species. The schematic diagram of hexagonal and cubic crystal GaN structures are shown in Figure 2.2 and Figure 2.3.

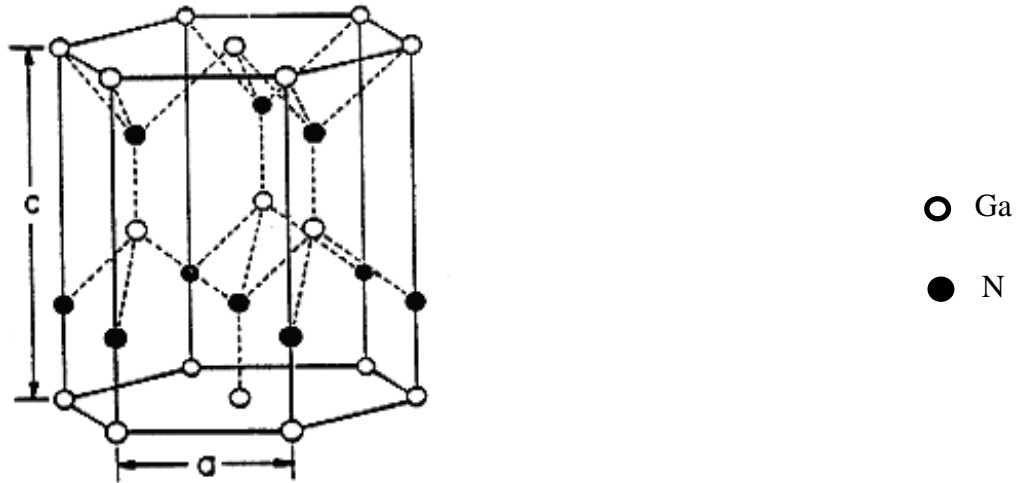


Figure 2.2 Hexagonal wurtzite crystal structure of GaN. The full circles are N, and open circles are Ga atoms. Adapted from (Edgar, 1994).

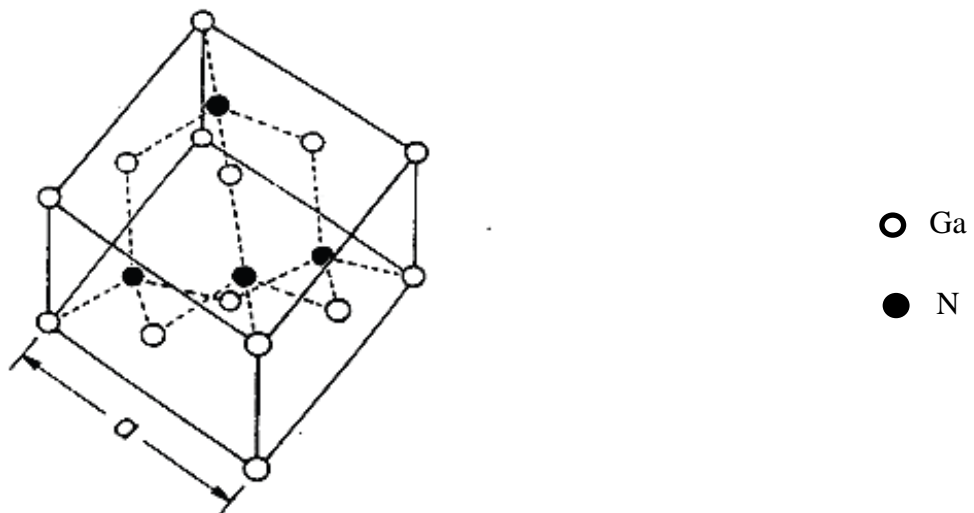


Figure 2.3 Zinc-blende crystal structures of GaN. The full circles are N, and open circles are Ga atoms. Adapted from (Edgar, 1994).

Table 2.1 summarizes the physical properties of GaN material for both wurtzite and zinc-blende GaN structures. The hexagonal wurtzite GaN structure is stable compared to the cubic zinc-blende GaN structure and both structures require different growth conditions. For cubic GaN, the growth process is more challenging where certain approaches are needed in order to obtain high purity structure due to its

metastable nature. The lattice constants for both structures are shown in Table 2.1. It is noted that, the amount of strain in the material will affect the lattice constants. The lattice constant will experience the compressive strain if it is smaller than the theoretical value. On the other hand, the lattice constant will experience tensile strain if it is higher than the theoretical value (Darakchieva et al., 2003).

Table 2.1 Physical properties of both hexagonal and cubic GaN (Church et al., 2018; Menniger et al., 1996; Kukushkin et al., 2008)

<b>Properties</b>	<b>Hexagonal GaN</b>	<b>Cubic GaN</b>
<b>Structure</b>	wurtzite	Zinc-blende
<b>Stability</b>	Stable	Metastable
<b>Energy band gap (eV)</b>	3.4	3.2
<b>Lattice constant (Å)</b>	$a = 3.189 ; c = 5.185$	$a = 4.52$
<b>Melting Point (°C)</b>	2500	2500
<b>Thermal conductivity (W/cm.K)</b>	2.1	2.1
<b>Thermal expansion Coefficient (1/K)</b>	$5.59 \times 10^{-6}$	N/A
<b>Thermal diffusivity (cm<sup>2</sup>/s)</b>	$\alpha_a = 3.17 \times 10^{-6}$	
<b>Heat capacity (J/mol)</b>	0.43	0.43
<b>Dielectric constant (static)</b>	35.3	35.3
<b>Refractive index</b>	8.9	9.7
<b>Bulk modulus (GPa)</b>	2.3	2.3
	210	210

Different techniques have been used to synthesize GaN nanostructures in different structures like rods, wires, tubes and etc. These techniques can be classified into two types: the catalyst-assisted and the catalyst-free techniques. The catalyst-assisted growth technique is usually used by a vapor-liquid-solid (VLS) process. By using metal catalysts by metal-organic vapour phase epitaxy (MOVPE) method

(Koester et al., 2010), most of GaN nanowires are usually obtained, while nanorods was obtained by MOCVD technique (Chae et al., 2015). Different types of morphologies were observed in the growth of nano/micro scale 1D nanostructure in MOCVD, such as kinked, branched, sidewall faceted and tapered.

GaN were grown on Si with several vapor-phase techniques. High quality of GaN on Si was grown with MBE (Calarco et al., 2007), MOCVD (Calarco et al., 2007) and HVPE (Paskova et al., 2004). However, all of these vapor-phase techniques are expensive and having complicated growth parameters. Consequently, relatively cheap and simple, RF sputtering and ECD techniques were introduced to grow the GaN.

Nowadays, GaN/Si heterostructure can be produced by using a simple nitridation technique (Yam et al., 2009) where the GaN layer can be produced by thermal annealing the sample under the ammonia ambient. Iskandar et al., (2006) reported that the growth temperatures and the concentrations of ammonia solution can affect the quality of GaN. Fong et al., (2013) performed the study on the effects of nitridation process on the growth of GaN thin films on p-type silicon substrates prepared by using spin coating method. In summary, nitridation technique plays an important role in improving the crystalline quality and in the synthesis of GaN nanostructures.

III-V nitrides semiconductor have received a lot of attention since they have special electronic and optical behavior and make them desirable for demand in electronics and optoelectronics devices (Cordier et al., 2010). Between the nitride compounds, GaN is the most intensely for studies material optical devices, because of its direct and wide band gap semiconductor of 3.4 eV. However, there are some issues



related to the growth of GaN on Si substrate. With a large lattice mismatch (17%) and a large difference of heat expansion coefficient (>100%), these problems have caused GaN to be difficult to grow on Si. Typically, different density of dislocations and cracks can be detected on GaN/Si interface and PSi becomes the best option to reduce the problems. This porous substrate will keep its crystalline character and has a porous structure that can reduce the thermal strain and controlling the creation of dislocations and cracks in GaN layers (Boufaden et al., 2003; Chaaben et al., 2004).

Generally high mobility of dislocations in the materials caused rapid degradation of all devices that have been created so far. In comparison, GaN-based devices work well without the effects of aging with high dislocation densities as  $10^{10}$  cm<sup>-2</sup>. Therefore, silicon-based optoelectronic technology with a small, high-resolution potential and full colour display, resulting in the integration of the Si and GaN based devices on the same chip makes it more practical (Krost & Dadgar, 2002).

## **2.5 Principles of Electrochemical Etching**

Electrochemical etching of the semiconductor is a technique of the anodic dissolution process applied both electrical and chemical responses (Kim & Cho, 2012). Light generation of electrons and holes are among the techniques used to support electrochemical reactions between semiconductor and liquids, called as electrolytes. Once a semiconductor is dipped in a chemical electrolyte, the current flows and the electrons are exchanged along the surface of the semiconductor and the electrolyte due to the difference of Fermi levels in the semiconductor and the electrolyte. In the electrochemical etching process, by using a power supply, the potential of the semiconductor substrate is measured. At the same time, its photon energy source is much higher than semiconductor band gap energy. This illuminates

the surface of the semiconductor and produces the formation of electrons and holes. The electrons and holes formed in the area of space charge near the surface are transported by two mechanisms: drifting under the influence of electric field, and dispersal due to the gradient of carrier concentration. These mechanisms promote semiconductors electrochemical etching.

### **2.5.1 Electrochemical Etching Mechanism of Porous Silicon**

PSi was discovered by Uhlir, (1955). Researchers are trying to develop electrochemical techniques for silicon wafers used in microelectronic circuits. This technology has attracted high interest for various potential applications including optoelectronic, photonics and bio sensing devices (Rusli et al., 2013). PSi is usually produced by anodic electrochemical etching method. This process is usually performed in aqueous or ethanoic hydrofluoric acid (HF) (Chudley & Greeno, 2012) and the pore structures were produced on the Si surface. This process involves the mixing of electronic and chemical factors. Porous structure also promote great surface region to volume ratio that would lead a better external efficiency devices like light-emitting-diodes (LEDs). To produce a uniform pore on the Si surface, an electrochemical anodization system has been used since this system can produced more uniform pores (Naderi & Hashim, 2012). The uniformity of the porous layer is controllable by adjusting several parameters, sch as current density, shape of current, the duration of etching, and electrolyte composition.

The creation of PSi structure, including Si-Si, Si-H, Si-O, and Si-F reactions on the Si surface. Table 2.2 shows the comparative strengths of these bonds, gained after the measurements of the molecular analog thermodynamics. However, the strength of these bonds does not play an important role for the stability of each

species on the surface of the silicon compared to the electronegativity of elements which is playing a more important role in the etching process. In aqueous solution, the Si-H and Si-C species tend to move to the surface of silicon, while the Si-F bond is highly reactive. Electronegative elements such as O and F form more polar Si-X bonds, making silicon atoms vulnerable to nucleophilic attacks. The surface of freshly prepared PSi is covered with a passivating layer of Si-H bonds, with minor quantities of Si-F and Si-O. In order to produce porous silicon, Si-F bond is the strongest bond that drives to the main chemical dissolution reaction (Chudley & Greeno, 2012).

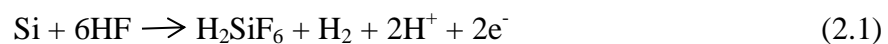
In the electrochemical reaction process, two electrodes are required to complete the electrical circuit and to maintain the neutrality of the charge. An electrode will supply electrons to the solution (cathode) and while the other electrode will remove the electrons from the solution (anode). In this process, holes are required for both electropolishing and pore formation. The electrochemical reaction that occurs at the platinum electrode is primarily the reduction of protons to hydrogen gas. Photons lead to the formation of electron/hole couples that will continue to engage in electrochemical dissolution.

Table 2.2 Enthalpies of some Si-X bonds.

Compound	Bond	Enthalpy, kcal mol <sup>-1</sup>
Me <sub>3</sub> Si-SiMe <sub>3</sub>	Si-Si	79
Me <sub>3</sub> Si-CH <sub>3</sub>	Si-C	94
Me <sub>3</sub> Si-H	Si-H	95
Me <sub>3</sub> Si-OMe <sub>3</sub>	Si-O	123
Me <sub>3</sub> Si-F	Si-F	158

Taken from Robin Walsh, Gelest Catalog: [www.gelest.com](http://www.gelest.com)

The porosity process is proposed by the hole generation located on the surface of Si-H bond (Santinacci & Djenizian, 2008). Holes ( $h^+$ ) are needed in both electropolishing and pores formation process. In this process, two hydrogen atoms will evolve for each Si atom to be disposed of. Therefore, for the pore formation process, current efficiency is due to two electrons of each Si atom dissolved and four electrons are required for the electropolishing regime (Beale et al., 1955; Bisi et al., 2000). The chemical reaction for pore formation and electropolishing process was summarized as below:



H<sub>2</sub>SiF<sub>6</sub> is the last product to be produced. It is stable and can be dissolved easily in solution and during pore formation. During this process, two of the four electrons will take part in the transfer of the interface charge, while the other two electrons undergo corrosive hydrogen emission. On the contrary, during electropolishing, four

electrochemically active electrons (Miranda et al., 2008; Mitani, 1990) offered different dissolution mechanism based on surface bonded oxidization scheme, with the subsequent capture of the electron and the subsequent electron injection, leading to the division of Si oxidization state. Hydride bond Si passivated the surface where hydrogen gas contributes to the expansion of the porous layer after the release of the potential used for a sufficient amount of time. In addition, the presence of Si-H surface bonds during PSi formation has been confirmed by several spectroscopic techniques (Venkateswara et al., 1991; Peter et al., 1988).

### **2.5.1(a) Direct Current Etching**

Photoelectrochemical etching technique is an interesting system for fabricating PSi layer. The PSi can be made more easily and uniformly by using this technique (Ali et al., 2008). The porosity, thickness, and pore diameter of PSi are fully dependent on the anodization settings, including HF concentration, anodization time, wafer type and resistivity, temperature, illumination, ambient humidity, current density and drying conditions (refer to Table 2.3). The response will be below ionic mass transfer control if the current density above the value. This will lead to changes in surface holes and to a smoothing of silicon layer (D. Zhang & Alocilja, 2008). At the current peak density, the actions will turn out to be PSi freestanding layers. When the density of current rises above the critical value, it will produce PSi film detachment from the Si substrate.

Table 2.3 Effects of anodization parameter on PSi formation (Bisi et al., 2000).

<b>An increase of ... yield a</b>	<b>Porosity</b>	<b>Etching rate</b>	<b>Critical</b>
Current density	Increase	Increases	-
HF concentration	Decreases	Decreases	Increases
Anodization time	Increases	Almost constant	-
Temperature	-	-	Increases
Wafer doping (p-type)	Decreases	Increases	Increases
Wafer doping (n-type)	Increases	Increases	-

The general method used for producing the PSi layer is the direct current (DC) electrochemical etching technique of Si substrate in HF-based electrolyte (Canham, 1990). During the anodic DC etching process, silicon fluoride (Bisi et al., 2000) will move and deposit at the end of pore tip. Hydrogen bubbles will adsorb on the Si pillar surface due to tension between the surface and obstructing the Si pores and thus reduce the HF concentration in the pores while the bubbles reduce the etching speed, resulting in shallow pores (Lehmann, 1993).

### 2.5.1(b) Pulsed Current Etching

Pulsed-current etching technique is a preferable technique for fabricating PSi substrate. During the pause time ( $T_{\text{off}}$ ), the pulsed-current allows the process to produce hydrogen gas bubbles and allow fresh HF species to penetrate and react with the silicon wall. Therefore, increase the rate of PSi etching (Naderi et al., 2013). Then  $T_{\text{off}}$  and time on,  $T_{\text{on}}$  will vary together with varying cycle time.

The current burst model (Carstensen et al., 2000) explained the development of pulse-current etching technique. The difference mechanism of pore formation was shown by this model. The basis in which the sequence of PSi formation is given as follows in Figure 2.4:

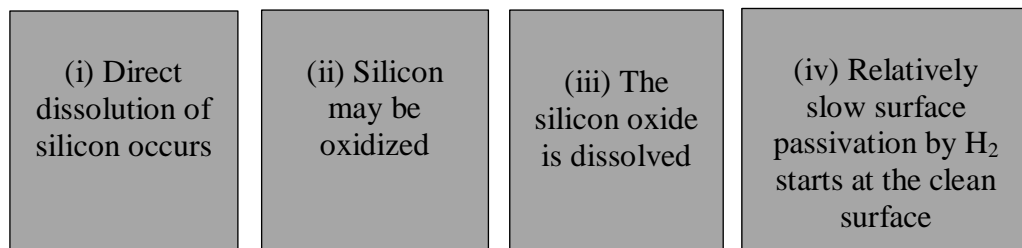


Figure 2.4 Basis sequence of PSi formation

To start the cycle again, each current burst needs to overcome this H-passivation. The current is required only in (i) and (ii). After the silicon oxide was dissolved; the free surface of the oxide tends to be completely covered with strongly bonded hydrogen and then is passivated. The complete process of H-passivation takes a lot of time; the time and perfection of this process depends largely on the orientation of the surface crystallographic (Kolasinski et al., 1995; Santos et al., 2014). The (100) surface requires the longest amount of time while the (111) surface takes the shortest time for complete coverage and thus passivation. Hence, by changing the  $T_{\text{off}}$ ,

different PSi structures can be formed. Actually the pause time was randomly used during the pore formation process, which means it can affect any of the four steps of the process. It is believed that, the pause time affects the process either directly by stopping the dissolving and oxidation measures, making H-passivation a dominant measure, or indirectly by refreshing the HF based electrolyte as mentioned earlier.

Controlled etching in the active dissolution regime is important and is possible through DC mode or pulsed current mode (Shiozaki, et al., 2006). When  $T_{on}$  is in pulsed current state, the voltage is switched on and the current increase dramatically as the substrate is dissolves into the electrolyte in the form of oxide (active dissolution). In the presences of an electrolyte system, it appears to be a barrier to diffusion that prevents the dissolution process. This is providing an opportunity for solid state film growth comprising oxide. This is called an active passive transition during the oxide layer thickness will continue to increase as long as the system is in  $T_{on}$  mode. The voltage is required in the transport of ionic species through the oxide layer and increases the proportion of oxide thickness and cause the system to experience a decrease in the current flow exponent. Reducing the  $T_{on}/T_{off}$  ratio, it will prevent the formation of oxide layers. Under this condition, the etching reaction will be continued in  $T_{on}$  mode followed by long periods of  $T_{off}$  mode, which allows the removal of anodic reaction products that are highly concentrated from the surface area by diffusion. Therefore, in this respect, the  $T_{on}/T_{off}$  ratio should be selected for sufficient product removal.

Amran et al., (2012) reported on the role of  $T_{off}$  on cation of PSi template for Au nanoparticles by using the integrated electrochemical technique. PSi was produced using a mixture of electrolyte of aqueous HF 49% and ethanol ( $C_2H_5OH$ ) 97% with ratio of 1:4. PSi was etched using pulse current etching technique with peak current



density  $10 \text{ mA/cm}^2$  and  $T_{\text{off}}$  at 2, 4, and 6 ms with the  $T_{\text{on}}$  fixed at 14 ms. From the result, a uniform distribution pores was observed with high visible PL intensity when  $T_{\text{off}}$  was increased to 4 ms at  $T_{\text{on}}$  14 ms. This shows that, the ratio of  $T_{\text{on}}:T_{\text{off}}$  be is important characteristic that can improve the porosity of PSi substrate. Meanwhile, in this study,  $T_{\text{off}}$  at 4, 6, and 8 ms corresponding to  $T_{\text{on}}$  10, 8, and 6 ms were be used.

The output signal from power supply is used to feed current through the anodic etching circuit by adjusting for both cycle times of  $T$  and  $T_{\text{off}}$  as shown in Figure 2.5.

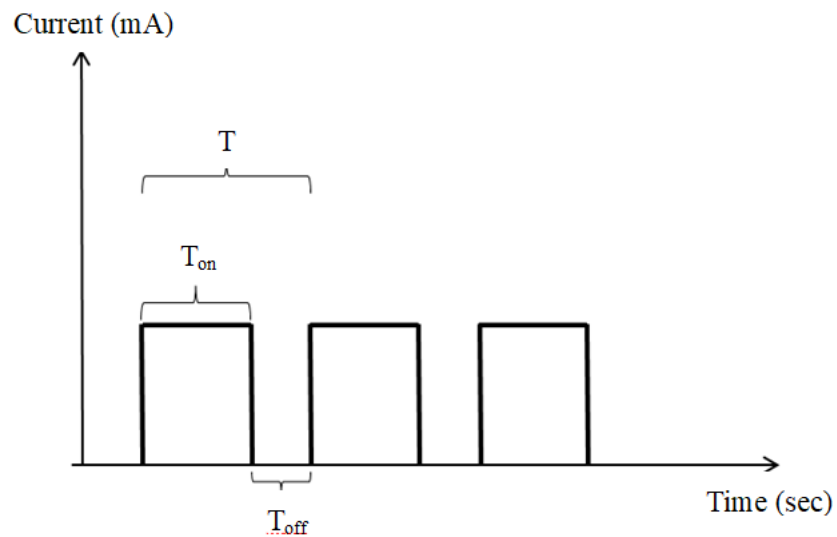


Figure 2.5 Schematic diagram of the waveform of the pulse current used in the etching process.

## 2.6 Principles of Electrochemical Deposition (ECD)

This technique is one of interesting techniques. In this technique, coating materials can be placed into another by donating electrons to ions in solution. Electrochemical deposition is a promising technique for use in preparing large area

electronic devices and many valuable applications keep being invented. This technique is also about the process in which the metal ions transform into solid metal and deposited on the cathode surface. This process is generated when an applicable amount of electric current passes through the electrolyte that containing the charged ions. In this study, the deposition was treated from the aqueous solution. The reduction of metal ions  $M^{z+}$  in aqueous solution is shown in Eq.2.3.



These deposition techniques are required for the research and development of electronic device technology, and valuable applications continue to be made. This technique have some advantages compared to other techniques which is, the surface thickness and morphology can be controlled due to less number of growth parameters, experimental setup is low-price, and the process may be available at low temperatures (Al-Heuseen, et al., 2010). Besides that, ECD technique is far less hazardous to the environment than existing methods such as MOCVD, MBE, HVPE, and ECD makes doping of the impurities easy (Katayama & Izaki, 2000; Al-Heuseen, 2011). Generally, electrochemical deposition technique is limited to the depositions of metal. But, many complex materials such as metal alloys, metal compounds and semiconductor materials deposition processes are widely used and established since the electrochemistry technology is growing and increasing with time.

### **2.6.1 Electrodeposition of Semiconductors**

This technique appears to be one of the easiest and most attractive method in the manufacture of thin films and nanostructure. Electrochemical deposition of semiconductor materials represents new challenges, as this technique exhibits attractive features in semiconductor field. With lower cost materials and can be